

Experimental observation of nonlinear Thomson scattering

Szu-yuan Chen, Anatoly Maksimchuk & Donald Umstadter
*Center for Ultrafast Optical Science, University of Michigan, Ann Arbor, MI
 48109, USA*
 (December 2, 2024)

A century ago, J. J. Thomson¹ showed that the scattering of low-intensity light by electrons was a linear process (i.e., the scattered light frequency was identical to that of the incident light) and that light's magnetic field played no role. Today, with the recent invention of ultra-high-peak-power lasers² it is now possible to create a sufficient photon density to study Thomson scattering in the relativistic regime. With increasing light intensity, electrons quiver during the scattering process with increasing velocity, approaching the speed of light when the laser intensity approaches 10^{18} W/cm². In this limit, the effect of light's magnetic field on electron motion should become comparable to that of its electric field, and the electron mass should increase because of the relativistic correction. Consequently, electrons in such high fields are predicted to quiver nonlinearly, moving in figure-eight patterns, rather than in straight lines, and thus to radiate photons at harmonics of the frequency of the incident laser light³⁻⁹, with each harmonic having its own unique angular distribution⁵⁻⁷. In this letter, we report the first ever direct experimental confirmation of these predictions, a topic that has previously been referred to as nonlinear Thomson scattering⁷. Extension of these results to coherent relativistic harmonic generation^{10,11} may eventually lead to novel table-top x-ray sources.

In this experiment, we used a laser system that produces 400-fs-duration laser pulses at 1.053- μ m wavelength with a maximum peak power of 4 TW. The 50-mm diameter laser beam was focused with an f/3.3 parabolic mirror onto the front edge of a supersonic helium gas jet. The focal spot is consisted of a 7- μ m FWHM Gaussian spot (containing 60 % of the total energy) and a large (> 100 μ m) dim spot. The helium gas was fully ionized by the foot of the laser pulse. A half-wave plate was used to rotate the axis of linear polarization of the laser beam in order to vary the azimuthal angle (ϕ) of observation. We define $\theta = 0^\circ$ as along the direction opposite to that of the laser propagation and $\phi = 0^\circ$ as along the axis of linear polarization. In a linearly polarized laser field, electrons move in a figure-eight trajectory lying in the

plane defined by the axis of linear polarization and the direction of beam propagation.

While the observation of harmonics in laser-plasma (or electron beam) interactions has been made by several groups¹²⁻¹⁶, that alone is insufficient to unambiguously identify nonlinear Thomson scattering and its underlying dynamics. Several other mechanisms might generate continuum or harmonics under our experimental conditions, and, therefore, need to be isolated and discriminated from the signal generated by nonlinear Thomson scattering: (1) continuum generated from self-phase modulation of laser beam in gas, (2) harmonics generated from atomic nonlinear susceptibility of gas or, especially, from the ionization process¹⁷, (3) continuum generated from (a) (relativistic) self-phase modulation of laser pulse in the plasma, or from (b) electron-electron bremsstrahlung and electron-ion bremsstrahlung, and (4) harmonics generated from the interaction of laser pulses with a transverse electron-density gradient¹⁴.

The main focal spot of the laser pulse undergoes relativistic-ponderomotive self-channeling when high laser power and gas density are used¹⁸. Side imaging ($\theta = 90^\circ$) of the 1st harmonic light (at the laser frequency) from nonlinear Thomson scattering shows that the laser channel has a diameter of < 10 μ m FWHM. However, interferograms¹⁸ show that the diameter of the plasma column is about 100-200 μ m, which is created by the wings with intensities $> 10^{15}$ W/cm² (the ionization threshold). Therefore, the light generated from laser-gas interaction should be observed to originate from the entire region of plasma, rather than from the narrow laser channel. Results of side imaging ($\theta = 90^\circ$ and arbitrary ϕ) of the 2nd and 3rd harmonics using a matching interference filter (10 nm bandwidth) show that the signal is emitted only from the narrow laser channel. In addition, the images of the harmonics have spatial distributions similar to the images of the 1st harmonic light, and their profiles vary in the same way as the laser power and gas density are changed. This rules out the possibility that the harmonic signal observed in the side images is a result of laser-gas interaction ((1) and (2)).

According to theory⁵⁻⁷, the harmonic signal generated from nonlinear Thomson scattering should have two important features: (1) it is linearly proportional to the electron density because it is an incoherent single electron process (the harmonics generated from a collection of electrons interfere with each other destructively, leaving only an incoherent signal, which is equal to the

single-electron result multiplied by the total number of electrons which radiate), and (2) it increases roughly as I^n , where n is the harmonic number, and gradually saturates when a_0 is on the order of unity⁷, where $a_0 = eE/m_0\omega_0c = 8.5 \times 10^{-10}\lambda[\mu\text{m}]I^{1/2}[\text{W}/\text{cm}^2]$ is the normalized vector potential, E is the amplitude of laser electric field, and $I = cE^2/8\pi$ is the laser intensity. These are characteristically different from the behavior of any other mechanisms. For instance, bremsstrahlung radiation should be proportional to the square of gas density ($N_e \cdot N_e$ or $N_e \cdot N_i$). In this experiment, the intensity of the harmonic signal was determined from the peak intensity or the average intensity of the images of harmonics, when it was plotted as a function of the observing angle, gas density and laser power. Both showed the same variations. Figure 1 shows the variation of the 2nd harmonic signal as a function of laser power and plasma (electron) density. The experimental results show a reasonable fit with the theoretical predictions. The 1st and 3rd harmonics show the same match with the theory.

Although the above two observations are consistent with nonlinear Thomson scattering as the source of the harmonic signal, the observation of the unique angular patterns is necessary in order to prove that the detailed dynamics of nonlinear Thomson scattering are indeed the same as the theoretical prediction. Figure 2(a) shows the ϕ -dependence of the 2nd harmonic signal at $\theta = 90^\circ$. The experimental results match qualitatively with the theoretical prediction, both having a quadrupole-type radiation pattern, which is characteristically different from the dipole pattern for other mechanisms (1)-(4), and linear Thomson scattering. Other measurements such as the ϕ -dependence of the 2nd harmonic light at $\theta = 51^\circ$ (an “anti-dipole” pattern), shown in Fig. 2(b), and the ϕ -dependence of the 3rd harmonic light at $\theta = 90^\circ$ (a “butterfly” pattern), shown in Fig. 3, were also made, all showing reasonable matches between the experimental data and the theoretical predictions. Such angular radiation patterns directly prove that electrons do indeed oscillate with figure-eight trajectories in an intense (relativistic) laser field. The angular pattern of the 1st harmonic light (linear component) of nonlinear Thomson scattering is also included in Fig. 2(b) for comparison.

Measurements of the spectra of the harmonics show that each of the spectra of 2nd and 3rd harmonics contains a peak at roughly the harmonic wavelength and a red-shifted broader peak, as shown in Fig. 4. The red-shifted broader peaks are believed to be part of the harmonic spectra generated by nonlinear Thomson scattering, because they vary in amplitude proportionally with the corresponding unshifted harmonic signals when the gas density and the laser power are changed. It was expected that the spectra of harmonics should be broadened tremendously for electrons in a high-fluid-velocity plasma wave⁶. A fast-phase-velocity electron plasma wave (with a maximum fluid velocity of as large as $\sim 0.2c$,

where c is the speed of light in vacuum) excited by stimulated Raman forward scattering¹⁹ was observed in this experiment at high laser power and gas density. However, the fact that the spectral distribution of the harmonics was not observed to change significantly with variation of gas density and laser power, when the plasma wave amplitude was, indicates that such spectral structure has nothing to do with the collective drift motion of electrons in the plasma waves. Although the angular radiation patterns of the harmonics could also be affected by such a $0.2c$ fluid-velocity oscillation, the changes are not significant enough (compare the solid and dash lines in Fig. 2(a)) to be identified from the experimental data⁷. In other words, all measurements done in this experiment match qualitatively with the prediction of incoherent nonlinear Thomson scattering of electrons without drift motion; the results appear not to be affected by the existence of plasma waves, probably due to destructive coherent interference. The absolute scattering efficiency is measured to be 8×10^{-4} and 1×10^{-4} photons per electron per pulse for the 2nd and 3rd harmonics (including both the unshifted and red-shifted spectral components), respectively, at $\theta = 90^\circ$, $\phi = 50^\circ$, for an angle of collection of 7×10^{-3} steradians. These numbers match reasonably well with the theoretical predictions for incoherent nonlinear Thomson scattering, which are 8×10^{-4} and 5×10^{-4} , respectively.

In summary, the results reported here confirm for the first time several predictions of relativistic electrodynamic theory, which were formulated forty years ago, coincident with the invention of the laser. As predicted⁷, a century-old fundamental “constant,” the Thomson cross-section, is now shown to depend on the strength of light.

REFERENCES

1. Thomson, J. J. Conduction of electricity through gases. Cambridge University Press, Cambridge (1906).
2. Maine, P. *et al.* Generation of ultrahigh peak power pulses by chirped pulse amplification. IEEE J. Quantum Electron. **24**, 398-403 (1988).
3. Vachaspati Harmonics in the scattering of light by free electrons. Phys. Rev. **128**, 664-666 (1962).
4. Brown, L. S. & Kibble, T. W. B. Interaction of intense laser beams with electrons. Phys. Rev. **133**, A705-A719 (1964).
5. Sarachik, E. S. & Schappert, G. T. Classical theory of the scattering of intense laser radiation by free electrons. Phys. Rev. D **1**, 2738-2753 (1970).
6. Castillo-Herrera, C. I. & Johnston, T. W. Incoherent harmonic emission from strong electromagnetic

waves in plasmas. IEEE Trans. Plasma Sci. **21**, 125-135 (1993).

7. Esarey, E., Ride, S. K. & Sprangle, P. Nonlinear Thomson scattering of intense laser pulses from beams and plasmas. Phys. Rev. E **48**, 3003-3021 (1993).
8. Hartemann, F. V. & Luhmann, N. C. Jr. Classical electrodynamical derivation of the radiation damping force. Phys. Rev. Lett. **74**, 1107-1110 (1995).
9. Hartemann, F. V. High-intensity scattering processes of relativistic electrons in vacuum. Phys. Plasmas **5**, 2037-2047 (1998).
10. Esarey, E. *et al.* Nonlinear analysis of relativistic harmonic generation by intense lasers in plasmas. IEEE Trans. Plasma Sci. **21**, 95-104 (1993).
11. Esarey, E. & Sprangle, P. Generation of stimulated backscattered harmonic generation from intense-laser interactions with beams and plasmas. Phys. Rev. A **45**, 5872-5882 (1992).
12. Meyer, J. & Zhu, Y. Second harmonic emission from an underdense laser-produced plasma and filamentation. Phys. Fluids **30**, 890-895 (1987).
13. Basov, N. G. *et al.* Investigation of $2\omega_0$ -harmonic generation in a laser plasma. Sov. Phys. JETP **49**, 1059-1067 (1979).
14. Malka, V. *et al.* Second harmonic generation and its interaction with relativistic plasma waves driven by forward Raman instability in underdense plasmas. Phys. Plasmas **4**, 1127-1131 (1997).
15. Englert, T. J. & Rinehart, E. A. Second-harmonic photons from the interaction of free electrons with intense laser radiation. Phys. Rev. A **28**, 1539-1545 (1983).
16. Bula, C. *et al.* Observation of nonlinear effects in Compton scattering. Phys. Rev. Lett. **76**, 3116-3119 (1996).
17. Brunel, F. Harmonic generation due to plasma effects in a gas undergoing multiphoton ionization in the high-intensity limit. J. Opt. Soc. Am. B **7**, 521-526 (1990).
18. Chen, S.-Y. *et al.* Evolution of a plasma waveguide created during relativistic-ponderomotive self-channeling of an intense laser pulse. Phys. Rev. Lett. **80**, 2610-2613 (1998).
19. Le Blanc, S. P. *et al.* Temporal characterization of a self-modulated laser wakefield. Phys. Rev. Lett. **77**, 5381-5384 (1996).

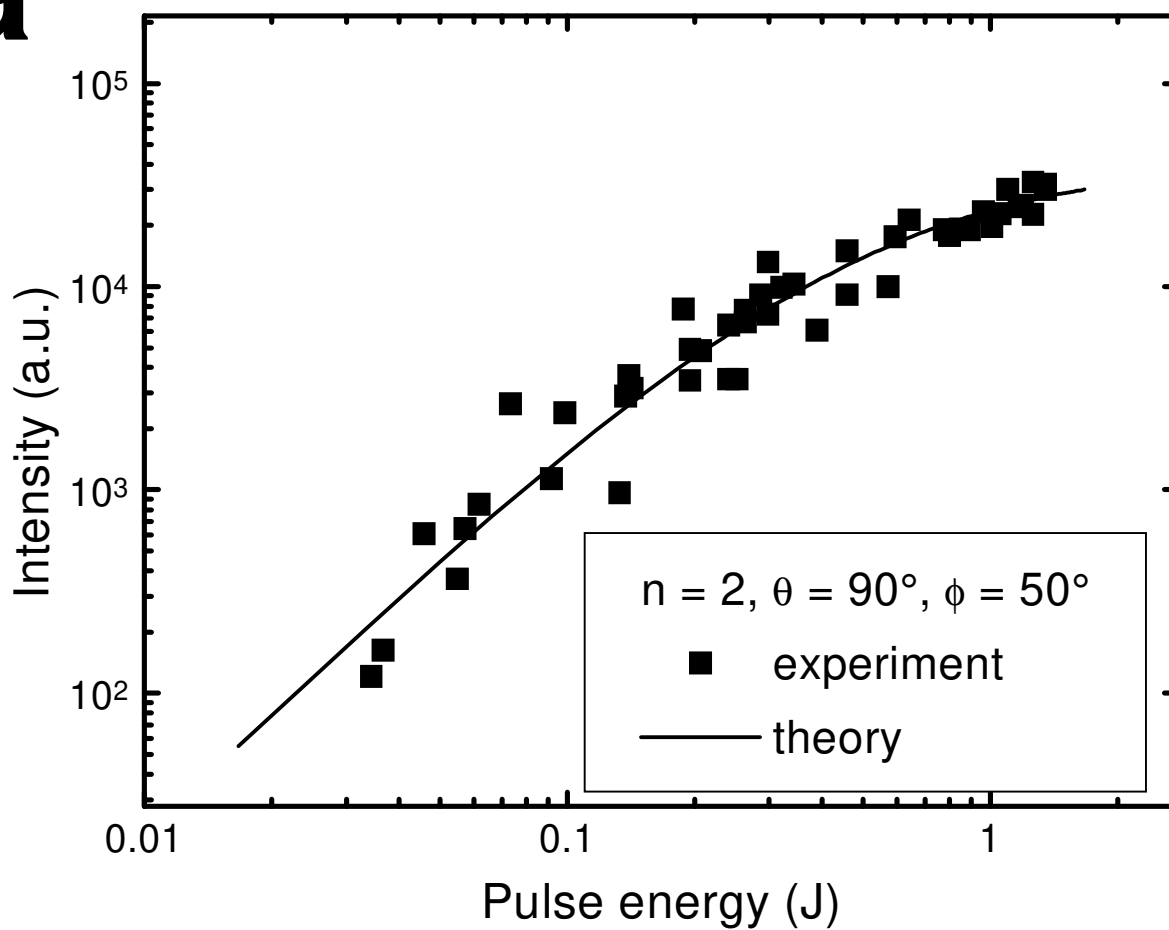
Acknowledgements This work was supported by U. S. National Science Foundation and the Division of Chemical Sciences, Office of Basic Energy Sciences, Office of Energy Research, U.S. Department of Energy. The authors would also like to thank G. Mourou, R. Wagner and X.-F. Wang for their useful discussions.

FIG. 1. Intensity of the 2nd harmonic light at $\theta = 90^\circ$, $\phi = 50^\circ$ (a) as a function of laser pulse energy at $6.2 \times 10^{19}\text{-cm}^{-3}$ electron density and (b) as a function of plasma electron density at 0.8-J laser pulse energy. (For 1-J laser pulse energy, the laser intensity is $4.4 \times 10^{18}\text{ W/cm}^2$ and a_0 is 1.88.) Each data point represents the result of a single laser shot. The theoretical predictions for zero drift velocity are plotted in solid lines for comparison. The only fitting parameter is just a constant for normalization in all figures. The laser pulse energy refers to the energy in the main focal spot. The inset shows the coordinate system used.

FIG. 2. Polar plots of the intensity of the 2nd harmonic light as a function of azimuthal angle (ϕ , in degrees) for 0.8-J pulse energy and $6.2 \times 10^{19}\text{-cm}^{-3}$ electron density at (a) $\theta = 90^\circ$ and (b) $\theta = 51^\circ$. The intensity is in arbitrary units. The solid circles represent the experimental data. The solid and dash lines represent the theoretical results for zero and nonzero drift velocity, $v = 0.2c$, in the laser propagation direction, respectively. The open circles and triangles represent the experimental data for the 1st harmonic signal taken at two different runs under the same conditions. The dotted line represents the theoretical result. Its dipole radiation pattern (peaked at $\phi = 90^\circ$) confirms that there is no depolarization effect in the plasma and that the collective effect of plasmas on the angular pattern is not significant (at least outside of a narrow cone along the axis of laser propagation). Although the data for $\phi = 180^\circ \sim 360^\circ$ are not plotted, it should be just a mirror image of the data for $\phi = 0^\circ \sim 180^\circ$ because of the intrinsic symmetry of the laser field, as predicted theoretically. Such symmetry has been verified in the experiment.

FIG. 3. Polar plot of the intensity of the 3rd harmonic light as a function of azimuthal angle (ϕ , in degrees) at $\theta = 90^\circ$ for 0.8-J pulse energy and $6.2 \times 10^{19}\text{-cm}^{-3}$ electron density. The intensity is in arbitrary units. The solid circles represent the experimental data. The solid line represents the theoretical result for zero drift velocity. The angular patterns of harmonics should not be sensitive to variation of laser intensity, as expected from theory and checked in the experiment. This is crucial to the success of our measurements because it alleviates the error caused by fluctuation of laser intensity.

FIG. 4. Spectra of the **(a)** 2nd and **(b)** 3rd harmonics at $\theta = 90^\circ$, $\phi = 50^\circ$ for 0.8-J pulse energy and $6.2 \times 10^{19}\text{-cm}^{-3}$ electron density. Vertical lines indicate the wavelengths of the unshifted 2nd and 3rd harmonics. The intensities are plotted in arbitrary units. The spectra do not change with variation of ϕ at any specific θ , so the angular distributions measured are not affected by the choice of filter bandwidth.

a**b**